# Single and Dual Band-Notch UWB Antenna Using SRR / CSRR Resonators

Zaid A. Abdul Hassain[1], Mustafa Mahdi Ali[1], and Adham R. Azeez[2]
1 Al-Mustansiriayah University, Faculty of Engineering, Baghdad, 10047 –Iraq
2 Uruk University, Faculty of Engineering, Baghdad, 10001- Iraq
Email: Zaidasaad_79@uomustansiriyah.edu.iq; mustafa_mahdi@uomustansiriyah.edu.iq; Adham.r.azeez@ieee.org

***Abstract***—In order for the interference of electromagnetic waves to be reduced in narrow band communications (WLAN, WiMAX and satellite communication), this paper presents a novel compact, low-cost, low-profile microstrip-fed line equipped with a single and dual band-notched ultra-wideband (UWB) patch antenna. A notched band is achieved at approximately 5.15-5.35 GHz and a 5.725-5.85 GHz that corresponds to WLAN IEEE802.11. To achieve this band notch band, an array of a four-element rectangular split ring resonator (SRR) is inserted into the neighbouring feed line. Moreover, in order to attain a WLAN band rejection and the 7.9-8.4 GHz X-band frequencies for satellite communication, three different sized complementary rectangular SRRs are etched in the ground plane,. The results led to the conclusion that the proposed antenna can be deemed a suitable candidate for applications of UWB communication having the property of single and double band notches.

***Index Terms***—WLAN, X-band, SRR, CSRR, ultra-wideband (UWB) antenna, band notch

## I. Introduction

The ultra-wideband (UWB) 3.1-10.6 GHz spectrum was introduced by the US Federal Communication Commission (FCC) for use in commercial applications [1]. Currently, the UWB communication system is considered the most prolific wireless communication technology that is able to support high data rates (110-200 Mbps), possesses low power spectral density (not exceeding -41dBm/MHz), and has usage in short range (indoor) applications. For a UWB communication system, the essential part of the system is the antenna. It must therefore be compact, with a low profile, and able to encompass a frequency range of 3.1-10.6 GHz. Numerous researchers have continued to discuss and debate the design requirements. However, current narrowband communication systems such as WLAN (5.15-5.35 GHz and 5.725-5.85 GHz), WiMAX (3.3-3.8 GHz), and X-band satellite communication (7.9-8.4 GHz) are still a concern.

Different techniques were utilised to integrate UWB characteristics with band-notched behaviour. The technique with the most popularity utilises embedded half-wave folded slots within the radiator by implementing various shapes, such as U-shaped [2], [3], T-shaped [5], C-shaped [4], and [6] and arc-shaped [7], [8]. Another technique relies on parasitic slits [9], PIN diodes [11], and Split Ring Resonators (SRR) [10] to notch the WLAN. Tri-arm resonators were also utilised for dual notches in [12]. For dual-notches characteristics, Aanchal S presented two opposite U-shape slots.

Pendry et al. presented a Split Ring Resonator (SRR) that is sometimes called Negative Refractive Index Materials [13], [14]. SRRs refer to a couple of concentric annular rectangular rings that contain parts in them that are situated at opposite ends, as demonstrated in Fig. 1(a). A magnetic field (H) that is vertically applied to the square ring surface produces currents which, given the independence on the structure's resonant properties, force out a magnetic field that may decrease or enhance the incident field. On the other hand, one can obtain the complementary split ring resonator (CSRRs) by drilling SRRs in the ground. Fig. (1b) shows this process makeup with apertures.

(a) (b)

Fig. 1. (a) Square split ring resonator (SRR), and (b) complementary square split ring resonator (CSRR)

This paper applied two techniques to design a novel single and dual band-notched UWB antenna for X-band and WLAN satellite applications. The first technique utilised to obtain the band notch for IEEE802.11a frequency band, 5.15-5.35GHz and hyper line frequency band, 5.725-5.85 GHz by inputting a collection of a four-elements rectangular split ring resonator (SRRS) that is situated close to and around the microstrip feed line. On the other hand, one can represent the second technique by etching the ground plane with three of the complementary SRRS (CSRR) in order to achieve X-band satellite communication and WLAN rejection.

## II. Single Band-Rejection Based on SRR and CSRR Structures

As shown in Fig. 2, a four-element array of a rectangular SRR is situated symmetrically on the microstrip-fed line. Then, it is inserted in order to obtain

Manuscript received August 25, 2018; revised April 29, 2019.
doi:10.12720/jcm.14.6.504-510

the characteristics of the band-notch of 5.15-5.35 GHz and 5.725-5.85 GHz WLAN for IEEE802.11a.

The topology of the proposed antenna is demonstrated in Fig. 3. The antenna radiator refers to a rectangular patch that measures 30mm in width and 13.5mm in length. Feeding of the patch is done from 50 Ω microstrip line that has a width of 2.85 mm. On the other hand, the ground plane of the rectangular antenna shape measures Wg in width and 13.5 mm in length. Then, the antenna is symmetrically situated around the y-axis. The design and simulation of this antenna are done on 1.6 mm-thick FR4 substrate via the finite element method (FEM) EM-simulator HFSS. As shown in Table I, the Wp, Lp, Wg, Lg, and Lf values are tuned parametrically in order to obtain the features of UWB.

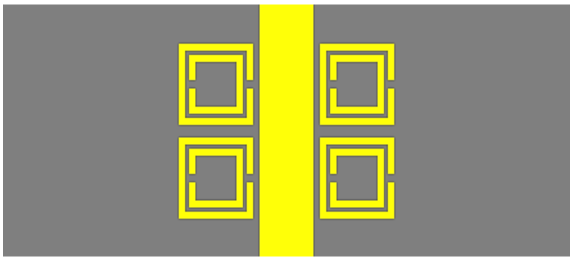

Fig. 2. The 4-Element Array of SRR

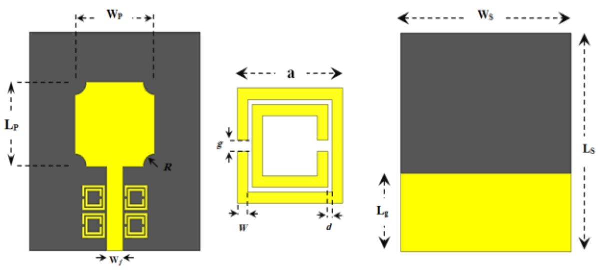


Fig. 3. The proposed antenna: (a) top view, (b) bottom view

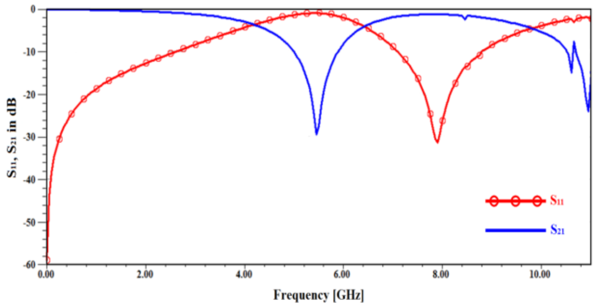


Fig. 4. S11 and S21 performance of the 4-element array of SRR.

Fig. 4 presents the scattered coefficients as S11 and S21. The results have demonstrated that the high scattering coefficient is obtained at 5.5 GHz as a resonance frequency (from 5.15 GHz to 6.1 GHz). Therefore, the band is presented as a rejected band.

Fig. 2 illustrates the first notched band technique utilised in this paper. The four rectangular SRR has a technique array that is etched in order to attain a single band-notched antenna structure found inside the WLAN band (5.15-5.85 GHz) and within the selected array dimensions, as demonstrated in Table I. Fig. 5 depicts the coefficient of reflection versus the frequency. The WLAN band contains the single band-notch. Fig. 6 illustrates the gain of the calculated antenna.

TABLE I: DIMENSIONS OF THE PROPOSED ANTENNA IN MM.

| Wp | LP | Lg | W*f* | Lf | LS | WS |
|---|---|---|---|---|---|---|
| 14 | 13.5 | 13.5 | 2.85 | 14 | 35 | 30 |
| R | a | w | d | s | g | D |
| 2 | 4 | 0.4 | 0.18 | 0.275 | 0.4 | 3.5 |

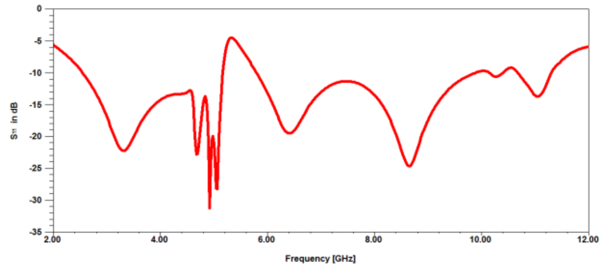


Fig. 5. The simulated S11 of the proposed antenna

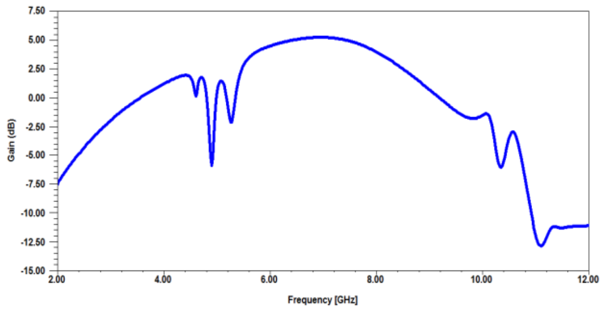


Fig. 6. The gain calculation of the proposed antenna

The CSRR structures are used to represent the other technique for rejecting the WLAN (4.85–6.1 GHz) band. The following dimensions were chosen for the CSRR cell: a= 4.75 mm, w= 0.475mm, d= 0.19mm and g=0.475 mm, where g refers to a split gap within one ring as illustrated in Fig. 7. To prevent any perturbation in the performance of the RL antenna and maintain the WLAN band rejection, there is a need to place the CSRR position at a distance of 2.4mm from the feed centre. All the simulations used the FR4_epoxy 4.4 substrate that measures 1.6 mm in height.

Fig. 8 presents the simulated scattering parameters of CSRR geometry. It was observed that the proposed CSRR dimensions proceeded with 4.7 GHz resonance frequency and a rejection bandwidth that goes from 4.5 to 4.9 GHz. Thus, the geometry of CSRR loaded microstrip feed can be used to obtain WLAN frequency band rejection for traditional antenna. This is demonstrated in Fig. 9.

So that the WLAN stopband can be obtained, there must be redistribution of the loaded CSRR in conventional antenna so that the maintenance of metamaterial cell performance can be ensured. Figure 10 shows the simulated scattering parameter (S11) for the conventional loaded antenna CSRR that comes before one stopband extending from 4.9 to 5.9, signifying WLAN band rejection. Furthermore, ghd RL performance of conventional antenna has been significantly influenced by the appearance of the undesirable band rejection (8 to 8.5 GHz reach to 10 dB). This issue will be solved later.

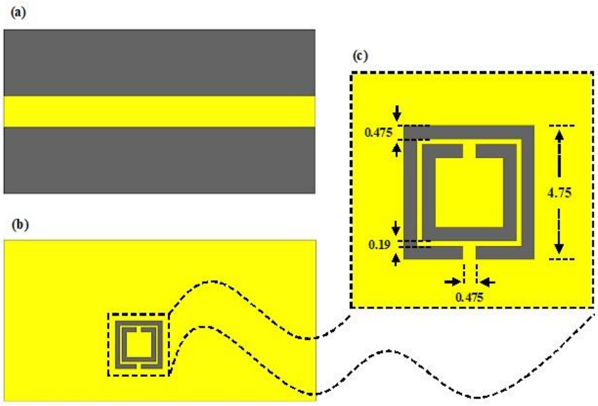


Fig. 7. Plane geometry of single CSRR cell loaded microstrip feed (a) top view (b) bottom view in mm

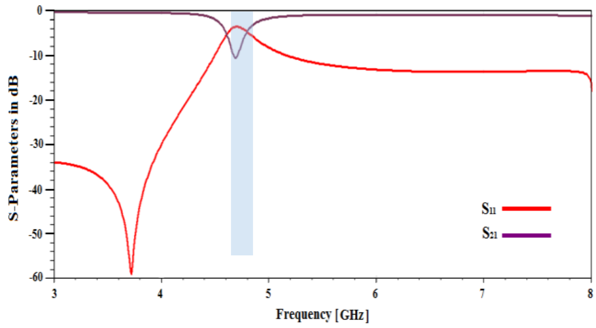


Fig. 8. Simulated scattering parameters of CSRR geometry

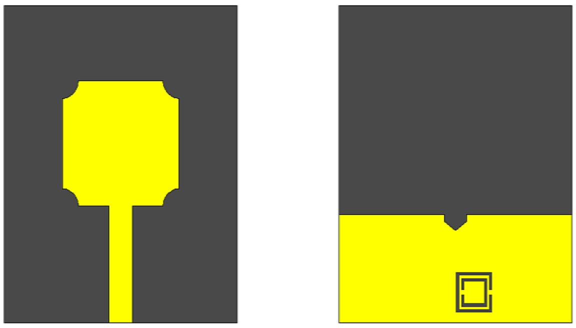

Fig. 9. Plane geometry of conventional antenna with CSRR loaded microstrip feed (a) top view (b) bottom view in mm

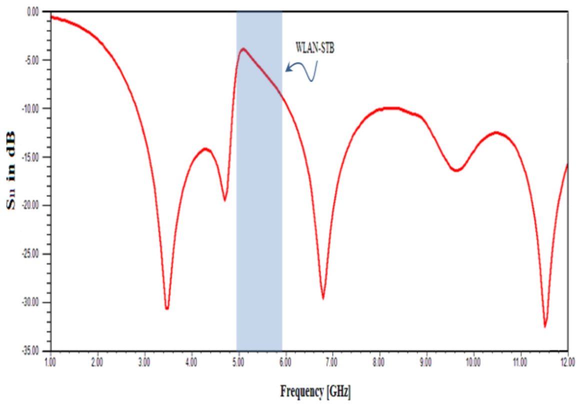


Fig. 10: Simulated scattering parameter S11 of conventional antenna with CSRR

## III. Double Band Rejection Based on CSRR Structures

For the X-band, two frequency ranges exist: uplink (7.9–8.4 GHz) and downlink (7.25-7.75 GHz). In order for all the bands to be covered, a parametric study is conducted for the single cell CSRR dimensions, in addition to utilising two cells. The measurements of the proposed CSRR cell were also set: a=3.2 mm, w=0.32 mm, d=0.128 mm and g=0.32 mm in order to maintain all X-band rejection and the RL performance of conventional antenna. As illustrated in Fig. 11, two proposed CSRR cells will be installed at a distance of 1.6 mm from the feed centre.

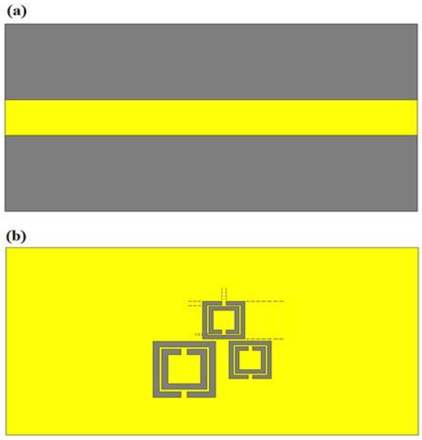


Fig. 11. Plane geometry of 3 CSRR cells loaded microstrip feed (a) top view (b) bottom view in mm

Fig. 12 presents the simulated scattering parameters for the geometry of the 3 CSRR cells loaded microstrip feed. Two stopband regions (STB-1 and STB-2) were observed. Creation of the first region took place as a result of the significant effect of the CSRR. Creation of the second region took place as a result of the effect of the combination of two CSRR cells. These cells have a 7.9 GHz resonance frequency and a rejection bandwidth that goes from 7.5 to 8.2 GHz (with 6dB $S_{11}$). The 3 CSRR cells loaded microstrip feed geometry can then be used to determine the WLAN frequency band rejection as well as the X-band rejection in conventional antenna. This is illustrated in Fig. 13. To prevent any RL antenna performance perturbations and simultaneously preserve WLAN band rejection and X-band rejection, 3 loaded CSRR cells need to be redistributed throughout the conventional antenna in a way so that the maintenance of the three metamaterial cell performances can be maintained. In Fig. 14, the simulated scattering parameter $S_{11}$ for the conventional antenna loaded 3 CSRR cells has one stopband that goes from 4.85 to 5.9 GHz. This is a representative of the WLAN band rejection, while the other stopband goes from 7.1 to 8.125 GHz. These are representatives of the downlink (7.25-7.75 GHz) and the majority of the uplink (7.9–8.4 GHz) X-band. Furthermore, there was a broad enhancement of the RL performance of the conventional antenna as a result of the loss of the undesirable band rejection (8 to 8.5 GHz reach to 10 dB) that was first observed during the loading of a single CSRR.

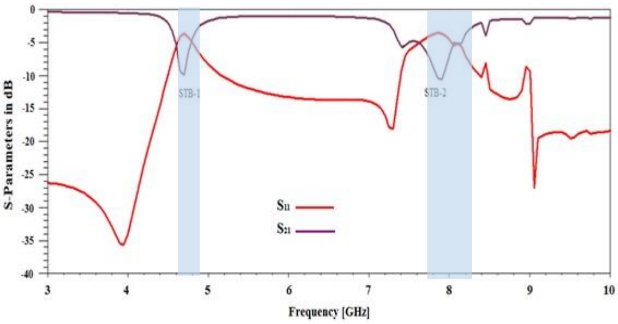


Fig. 12. Simulated scattering parameters of 3 CSRR cells loaded microstrip feed geometry

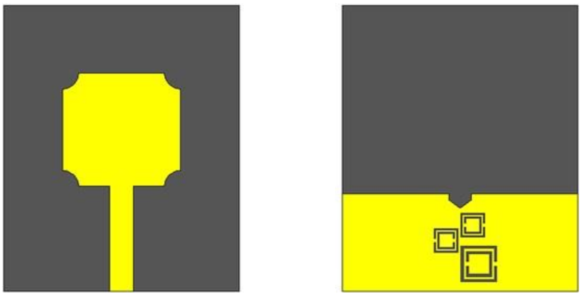

Fig. 13. Plane geometry of conventional antenna with 3 CSRR cells loaded microstrip feed (a) top view (b) bottom view in mm

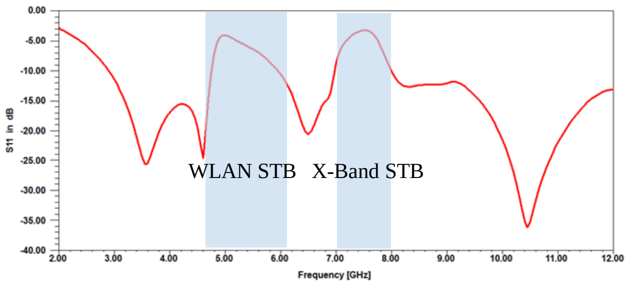


Fig. 14. Simulated scattering parameter S11 of conventional antenna with 3 CSRR cells loaded

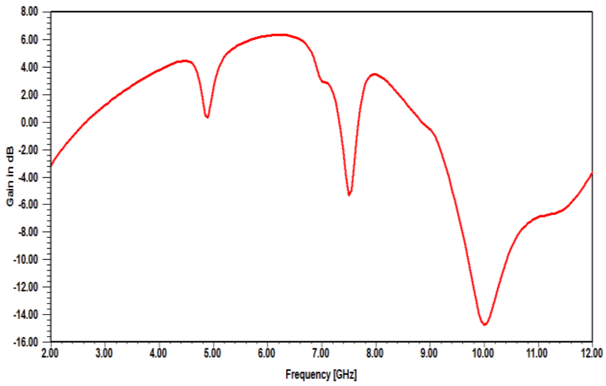


Fig. 15. Simulated summit gain response of conventional antenna with 3 CSRR cells loaded

Fig. 15 presents a simulated summit gain response that is indicative of the highest point that can be reached by the gain, 6.6dB at 6.4 GHz. A decent gain reduction was also observed at two central frequencies (0.46dB at 4.9GHz, and -4.9dB at 7.55GHz), for the two rejected bands as a result of the CSRR influence. Fig. 16 presents the efficiency of the two proposed antennas, UWB antenna based CSRRs and UWB antenna based SRRs. Extremely high radiation efficiencies, with a maximum of 95.5% and 94% for the first and second antenna, respectively, were observed in all frequency bands with the exception of the frequency band-notch. It therefore reduces the interference of the electromagnetic waves in X-band and WLAN for satellite communications. The radiation efficiencies' behaviour in the band-notch frequencies is a result of the insertion of the SRR and CSRR structures that results in the loss of the antenna matching within these bands.

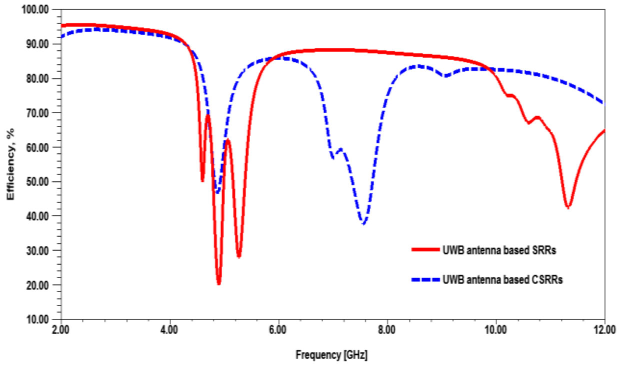


Fig. 16. Radiation efficiency of the both proposed antennas

Table II illustrates a comparison among the band-notch UWB antennas proposed in the study and other reported references. Data show that our proposed methods had better gain compared to other works presented in the table. The techniques utilised in this study are based on SRR and CSRRs arrays that are inserted beside/below the line of the feed. There was no observed change on the radiating patch. Thus, it can be said that gain and radiation stability were attained. On the other hand, the work in the references presented in Table II relies on the insertion of slots in the radiating patch. As a result, high degradation in the radiation and gain stability was observed.

TABLE II: COMPARISON OF BAND-NOTCH UWB ANTENNAS.

| Work | Size (mm2) | Technique that used to achieve the band notch | Gain (dB) |
|---|---|---|---|
| Ref.[15] | 26×35 | Pair of flexuous slots on the radiation structure for 3.5 GHz rejection band and C-shaped slot on the ground plane for 5.5 GHz band notch | 5.2 |
| Ref.[16] | 30×30 | A split ring slot in the radiator for 3.5 GHz band notch and two symmetrical slots in the ground plane for 5.5 GHz band notch | <5 |
| Ref.[17] | 35.5×30 | Arc H-shaped slot on the radiating patch for WiMAX band notch and couple of narrow slots on the ground plane for WLAN notched band | — |
| Ref.[18] | 31×31 | U-shaped inverted slot in the feed line for WiMAX band | <2.5 |

| | | | |
|---|---|---|---|
| | | reject and vertical up C-shaped slot in the radiating patch, for the WLAN rejection band | |
| Ref.[19] | 53.25×35 | Inverted U-shaped slot within the feeding line to reject (5.1–5.9) GHz band and four L-shaped lines near the antenna feeding line to reject the (8.2–10.0) GHz band | <6 |
| Our work | 35×30 | Array of a four element SRR near and around the microstrip feed line for 5.15-5.35 GHz and 5.725-5.85 GHz WLAN band notch | <6 |
| Our work | 35×30 | Three different sized CSRRs in the ground plane (below the feed line) for WLAN and (7.9-8.4) GHz rejection bands | >6.3 |

## V. Experimental Results

For substantiating the recommended design, the band notched antenna prototypes, UWB antenna based CSRRs and UWB antenna based SRRs are fabricated by deploying an LPKF ProtoMat S100, and FR4 substrates as depicted in Fig. 17. Both antennas were gauged by utilising the Agilent RF-Vector Network Analyser (VNA). Fig. 18 depicts the measurement setup for characterising the band notch by deploying the recommended structures.

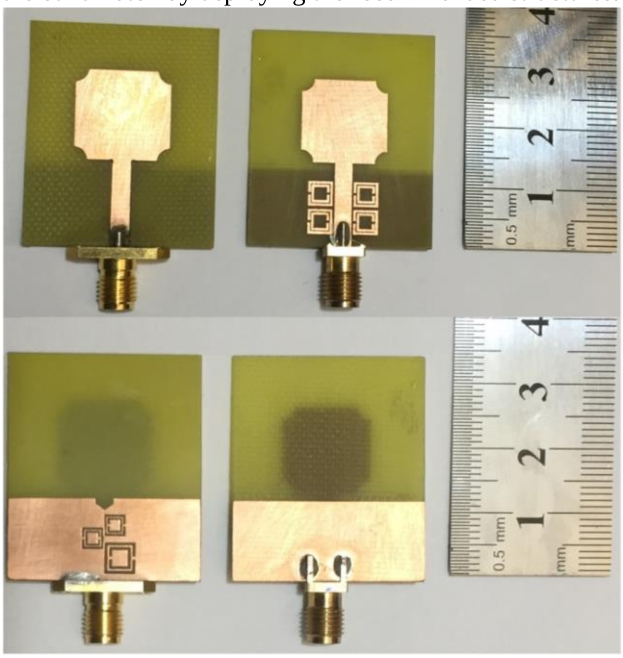

Fig. 17. Fabrication of UWB band notch antenna, (a) top view, and (b) bottom view.

Fig. 19 depicts the comparison between the simulation and measurement results of both band notch antenna structures with regards to $S_{11}$. Figures 20 and 21 exhibit the simulated as well as measured radiation far-field patterns of the recommended antennas in both E, H-planes at operation frequencies: 3.5GHz, 6.5GHz, and 10GHz. One can note a good agreement between the measured and simulated results with a marginal difference. This may be due to the SMA mismatch, fabrication error, and losses in SMA connector, substrate, and copper.

Fig. 18. Measurement setup for both UWB band notch antenna fabricated

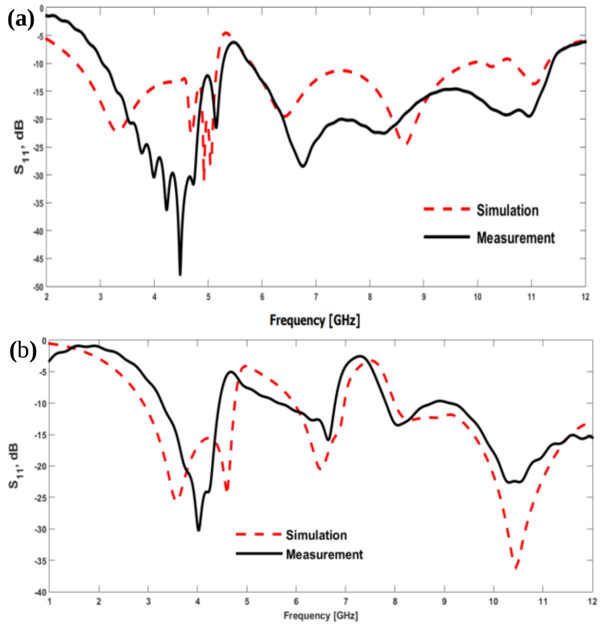


Fig. 19. Simulation and measurement results' comparison of both band notch antennas; (a) UWB antenna based SRRs and (b) UWB antenna based CSRRs

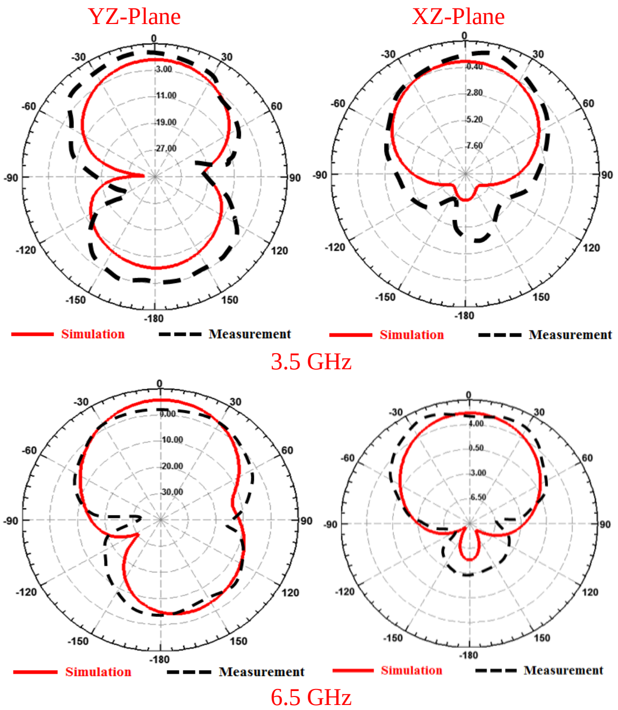

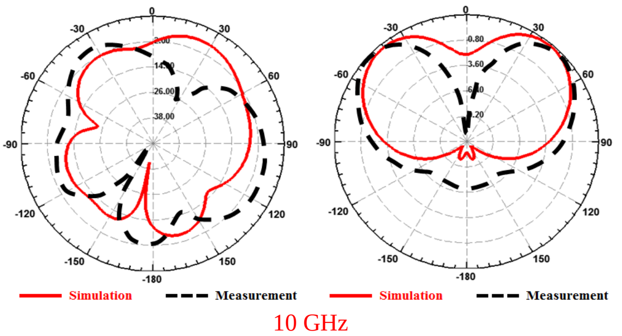


Fig. 20. Simulation and measurement radiation patterns of UWB antenna based SRRs at three different operating frequencies

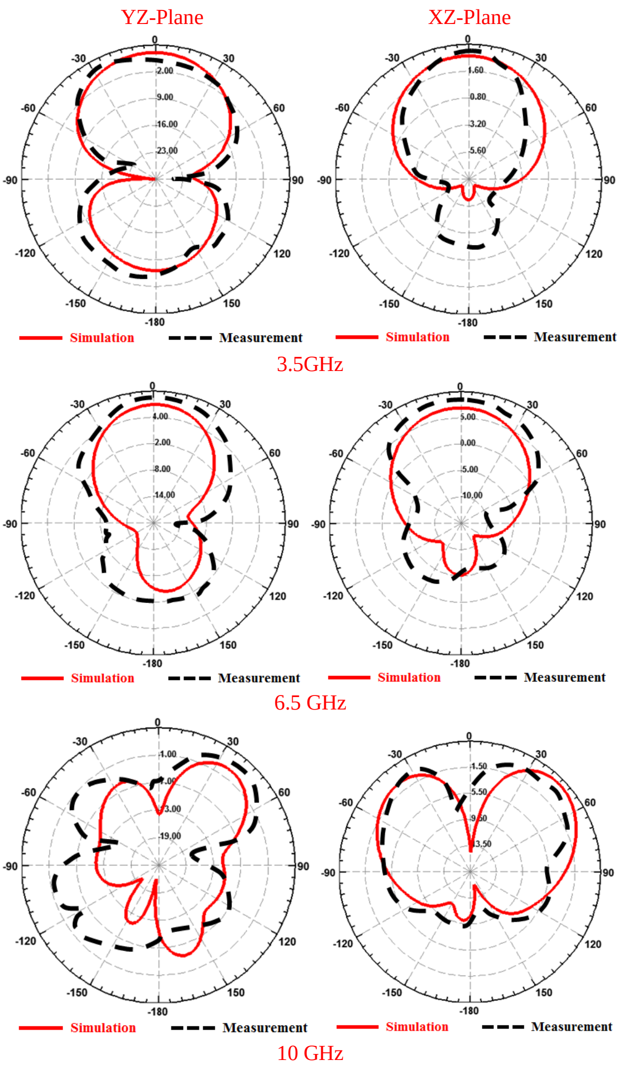


Fig. 21. Simulation and measurement radiation patterns of UWB antenna based CSRRs at three different operating frequencies

## VI. CONCLUSION

An innovative low-profile, compact, low-cost microstrip-fed line with a single and dual band-notched ultra-wideband (UWB) patch antenna was scrutinised. The notched band of about 5.15-5.35 GHz and 5.725-5.85 GHz WLAN for IEEE802.11a frequency band was attained by engraving out an array of a four-element rectangular split ring resonator (SRR) close to and around the microstrip feed line. Moreover, by engraving out three complementary rectangular SRRs of various sizes in the ground plane, the rejections for the WLAN and 7.9-8.4 GHz X-band frequencies for satellite communication were attained. The outcomes indicate the high-level agreement between the experimental data and simulation. This means that the conclusion of the recommended antenna can be considered as an apt contender for UWB communication applications.

## REFERENCES

[1] P. Li, J. Liang, and X. D. Chen, “Study of printed elliptical/circular slot antennas for ultra-wideband applications,” *IEEE Trans. Antennas Propg.*, vol. 54, no. 6, pp. 1670-1675, Jun. 2006.

[2] Y. J. Cho, K. H. Kim, D. H. Chio, S. S. Lee, and S. O. Park, “A miniature UWB planner monopole antenna with 5-GHz band-rejection filter and the time domain characteristics,” *IEEE Trans. Antennas Propg.*, vol. 54, no. 5, pp. 1453-1460, May. 2006.

[3] T. Dissanayake and K. P. Esselle, “Prediction of the notch frequency of slot loaded printed UWB antennas,” *IEEE Transactions on Antennas and Propagation*, vol. 55, no. 11, pp. 3320–3325, 2007.

[4] J. Y. Sze and J. Y. Shiu, “Design of band-notched ultrawideb and sequre aperture antenna with a hat shaped back-patch,” *IEEE Trans. Antennas Propg.*, vol. 56, no. 10, pp. 3311-3314, Oct. 2008.

[5] V. Sadeghi, C. Ghobadi, and J. Nourinia, “Design of UWB semi-circle-like slot antenna with controllable band-notch function,” *Electronics Letters*, vol. 45, no. 25, 2009.

[6] S. Natarajamani, S. K. Behera, and S. K. Patra, “Compact Slot Antenna for UWB Application and Band-Notch Designs,” in *Proc. IEEE International Conference on Computational Intelligence and Communication Networks*, Bhopal, India, 2010.

[7] T. A. Denidniand and Z. Weng, “Hybrid ultrawideband dielectric resonator antenna and band-notched designs," *IET Microwaves, Antennas & Propagation*, vol. 5, no. 4, pp. 450–458, 2011.

[8] M. Moosazadeh, A. M. Abbosh, and Z. Esmati, “Design of compact planar ultrawideband antenna with dual-notched bands using slotted square patch and pi-shaped conductor-backed plane,” *IET Microwaves, Antennas & Propagation*, vol. 6, no. 3, pp. 290–294, 2012.

[9] N. Ojaroudi and M. Ojaroudi, “Novel design of dual band-notches monopole antenna with bandwidth enhancement for UWB applications,” *IEEE Trans. Wireless Propagation Letter*, vol. 12, no. 11, pp. 698-701, May. 2013.

[10] R. Azim, M. T. Islam, and A. T. Mobashsher, “Design of a dual band-notches UWB slot antenna by means of simple parasitic slits,” *IEEE Trans. Antennas Propg.*, vol. 12, pp. 1412-1415, November. 2013.

[11] D. Sharker, K. V. Raivastava, and K. Saurav, “A compact microstrip-fed triple band notched UWB monopole

antenna," *IEEE Trans. Antennas Propg.*, vol. 13, pp. 396-399, 2014.

[12] M. S. Khan, A. D. Capobianco, M. F. Shafique, B. Ijaz, and B. D. Braaten, "Compact planar UWB MIMO antenna with on-demand WLAN rejuction," *IET, Electronic Letters*, vol. 51, no. 13, pp. 963-964, June 2015.

[13] A. Sharma and M. M. Sharma, "An UWB antenna design with dual band notched characteristic using U-shaped slots," in *Proc. IEEE International Conference on Signal Processing and Communication*, Noida, India, 2016.

[14] A. R. Azeez, T. A. Elwi, and Z. A. A. AL-Hussain, "Design and Analysis of a Novel Concentric Rings based Crossed Lines Single Negative Metamaterial Structure," *Elsevier, Engineering Science and Technology, an International Journal*, vol. 20, no. 3, pp. 1140-1146, 2017.

[15] Y. Zhu, F. S. Zhang, C. Lin, Q. Zhang, and J. X. Huang, "A novel dual band-notched monopole antenna for ultra-wideband application," *Progress in Electromagnetics Research Letters*, vol. 16, pp. 109–117, 2010.

[16] Z. A. Zheng and Q. X. Chu, "Compact CPW-FED UWB antenna with dualband-notched characteristics," *Progress in Electromagnetics Research Letters*, vol. 11, pp. 83-91, 2009.

[17] Ronghua Shi, Xi Xu, Jian Dong, and Qingping Luo, "Design and analysis of a novel dual band-notched UWB antenna," *International Journal of Antennas and Propagation*, 2014.

[18] A. Chaabane, F. Djahli, and S. Redadaa, "A dual-band-notched antenna for UWB communication systems using two different shaped slots," *Arabian Journal for Science and Engineering*, vol. 39, no. 8, pp. 6215-6223, 2014.

[19] B. T. Ahmed, E. M. Lasa, P. S. Olivares, and J. L. M. Campos, "UWB Antennas with multiple notched-band function," *Progress in Electromagnetics Research Letters*, vol. 77, pp. 41–49, 2018.

**Zaid Asaad Abdul Hassain** was born in Baghdad, Iraq, in 1979. He received the B.S. and the M.S. degree from the AL-Mustansiriyah University, Faculty of Engineering, Electrical Engineering Department, Iraq, in 2000 and 2003, respectively. His research interests include microwave and antenna.

**Mustafa Mahdi Ali** was born in Baghdad, Iraq, in 1984. He received the B.S. degree from the AL-Mustansiriyah University, Faculty of Engineering, Electrical Engineering Department, Iraq, in 2006 and the M.S. degree from the Yarmouk University, Faculty of Hijjawi for Engineering Technology, Department of Telecommunications Engineering, Jordan, in 2015.

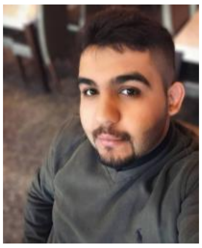

**Adham Rabea Azeez** was born in Baghdad, Iraq, in 1991. He completed B.S. from Al-Ma'mun University College, in Communications engineering, and the M.S. degree from AL-Mustansiriyah University, Faculty of Engineering, Electrical Engineering Department, Iraq, in electronic and communications engineering, in 2013 and 2017, respectively. In 2016, he became a member in the Iraqi Forum of Inventors. His research interests include microwave and antenna.